THE PENNSYLVANIA STATE UNIVERSITY
SCHREYER HONORS COLLEGE

DEPARTMENT OF CHEMISTRY

STUDY OF VARIATION IN REACTIVE SURFACE SITES AND ALTERATION LAYER PROPERTIES OF NUCLEAR WASTE GLASS USING SOLID-STATE NMR

DANIEL P. BANKS
SPRING 2014

A thesis
submitted in partial fulfillment
of the requirements
for a baccalaureate degree
in Chemistry
with honors in Chemistry

Reviewed and approved* by the following:

Karl T. Mueller
Professor of Chemistry
Thesis Supervisor

Raymond L. Funk
Professor of Chemistry
Honors Adviser

* Signatures are on file in the Schreyer Honors College.

ABSTRACT

The incorporation of nuclear waste materials into borosilicate glasses through the process of vitrification has been studied as a method for storing the harmful radioactive waste products produced from nuclear fuel processing. Borosilicate glasses are an ideal choice for the storage of nuclear waste materials due to their high chemical and thermal stability over the radioactive lifetime of the waste components. One of the primary concerns involving nuclear waste vitrification is the corrosion of these glasses in the presence of water. The focus of this study is to measure the chemical reactivity of these waste glass surfaces under different corrosion conditions such as pH, corrosion time, surface area, and glass composition. We quantify the chemical reactivity of these surfaces by measuring the number of lone Q^3 surface hydroxyls via attachment of the probe molecule 3,3,3-(trifluoropropyldimethyl)chlorosilane (TFS) and ^{19}F magic-angle spinning solid-state NMR analysis.

The glass samples examined in this study were the simulated waste glasses SA1R and SS2R which are modeled after the American AFCI and French SON68 waste glasses respectively. The results of our study show that the surface reactivity of these waste glasses depends on a number of different factors. We find that the chemical reactivity of these glasses increases as a function of increasing surface area and pH. We also observe a variation in the number of measured reactive surface sites as a function of increasing corrosion time. From the results of our study we also hypothesize that there are interactions occurring between the buffer components used in our corrosion solutions and the surface of our glass samples. If this is the case it may be possible that these buffer components used in glass corrosion experiments may block corrosion sites. However, further studies would need to be performed in order to confirm this hypothesis.

TABLE OF CONTENTS

LIST OF FIGURES

LIST OF TABLES

ACKNOWLEDGEMENTS

I'd like to start off by thanking Dr. Raymond Funk for serving as my honors adviser and helping to guide me through the process and requirements set forth by the honors college. I would also like to thank Dr. Carlo Pantano of the Penn State Materials Science and Engineering department whose generous funding support for me during the summer provided significant assistance in allowing me to complete this project. Genreal funding for the project was provided by the Nuclear Energy University Program (NEUP) under contract 00101956.

Finally, I would like to thank everyone in the Mueller research group for all of their help and support in the completion of this project. I would like to give an extra special thank you to Dr. Karl Mueller and Dr. Kelly Murphy. Dr. Mueller took me into the group when I was a junior and was always available to answer all of my questions in various aspects of my project, chemistry, and even life. I will certainly miss his helpful guidance and support as well as his always entertaining stories. Dr. Murphy was the best mentor I could have possibly asked for. She was always willing to take time out of her schedule to assist me with whatever questions I may have had regarding my project. Her generosity and support in the completion of my project, in addition to working on her own, without a doubt helped make this all possible.

Chapter 1

Introduction: Overview of Nuclear Waste Glass

1.1 Nuclear Waste Vitrification

1.1.1 Background

Since the development of nuclear power in the early 1950s, finding a way to safely store the by-products of the nuclear fission process has posed a challenge for scientists. The key to disposal of nuclear waste is finding a cost-effective, stable, and environmentally safe method for trapping, or immobilizing, the radioactive material. Nuclear waste can be separated into two categories based on the type of radioactive nuclides present in the waste. These categories are high-level radioactive waste (HLW), which is typically produced through nuclear reprocessing, and low-level radioactive waste (LLW), which contains radionuclides with lower activity. The main issue that arises with permanent storage is the need for stability for the duration of the waste's radioactive lifetime.

Several methods have been utilized for the immobilization of radioactive waste including cementation, bituminization (immobilization in asphalt), and vitrification (immobilization in glass). Vitrification in particular has been found to be an efficient and effective method for immobilizing nuclear waste due to the ability of glasses to store a wide range of radionuclides.[1] For over 50 years borosilicate glass has been studied as an option for containing nuclear waste due to its high chemical and thermal stability as well its ability to be easily processed on an industrial scale. We cannot, however, measure the behavior of these borosilicate glasses for the duration of the waste's radioactive lifetime and instead must rely on modeling their long-term

behavior. In the United States, construction on a vitrification plant at the Hanford Site in Washington has begun and operations are set to begin in 2019.[2]

1.1.2 Formation & Storage of Waste Glass

Nuclear waste products are incorporated into a glass matrix by mixing with glass forming components and melting at high temperatures. The primary type of glass currently used for nuclear waste vitrification is borosilicate glass. The specific composition of a glass is carefully chosen based on ease of preparation and chemical durability (resistance to corrosion). Factors considered in glass preparation include the melting temperature, the percent by mass of waste it can accommodate, and the radioactive level of the waste it contains. Typically these glasses must be formed at sufficiently low melting temperatures ($\leq$ 1500 K) to prevent volatilization of waste products, such as Cs and Sr, which become a source of additional contamination.[1]

Before melting, HLW and LLW must be separated in an attempt to better match the level of the waste's radioactivity with an appropriate glass composition. Once the waste is separated it is mixed into a slurry with silica and other glass forming materials before being passed into a high-temperature furnace where it forms a molten mixture. This mixture is then poured into metal containers where it is supercooled to generate a solid glass. The choice of material for these containers is critical because they must be able to withstand the high temperatures resulting from radioactive decay of the waste as well as protect the glass from environmental corroding agents. As such, cast-iron or stainless steel are often chosen. Once the container is sealed it is then decontaminated and transported to a deep underground burial site in an attempt to prevent any radiation from reaching the Earth's surface. A diagram of the nuclear waste vitrification process is displayed in Figure 1-1.

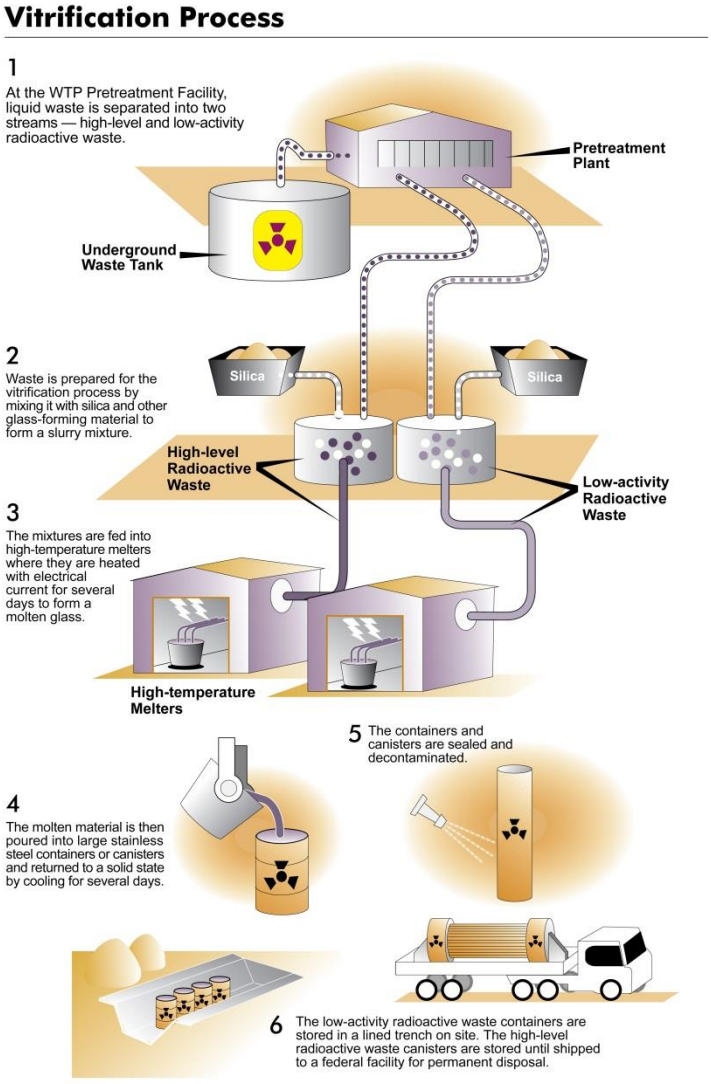

Figure 1-1. Diagram of the vitrification process from glass formation to storage.[3]

1.1.3 Corrosion Process

Although glass has incredibly high thermal and chemical stability, corrosion is possible especially over long periods of time. The corrosion of glass is an area of concern for implementation of vitrification of radioactive waste as a permanent storage technique due to the

potential loss of radionuclides to the environment. As such, a majority of the research focused on studying the long-term glass durability through reaction kinetics of the corrosion process.

The corrosion of waste glass is a complex, multi-step process depending on a number of different factors. The first stage of the corrosion process is known as interdiffusion (ion exchange). In the interdiffusion stage, a proton or hydronium ion in solution exchanges with an alkali metal (network modifying cation) within the glass:

$$\mathrm{Si-O^-\ \ Na^+ + H^+ \leftrightarrow Si-OH + Na^+}$$

When this occurs network-modifying cations within the glass network are released to solution, resulting in an increase in pH. This stage is also selective in that only network-modifying cations that are weakly bonded to oxygen can be exchanged. Interdiffusion can occur simultaneously with hydrolysis in which hydroxyls nucleophilically attack the glass network, resulting in the breaking of bridging oxygen bonds:

$$\mathrm{Si-O-Si + OH^- \leftrightarrow Si-OH + Si-O^-}$$

$$\mathrm{Si-O^- + H_2O \leftrightarrow Si-OH + OH^-}$$

The continued hydrolysis of the glass network eventually results in its breakdown. The corrosion mechanisms for interdiffusion and hydrolysis have been well documented in the chemical literature.[4]

After a sufficient amount of time has passed, the corrosion rate of some glasses (as measured by species lost to solution) decreases significantly. There are currently two hypotheses for why this happens. The first hypothesis is that as silicon is released to solution, the solution becomes saturated and reaches a thermodynamic equilibrium. The corrosion rate decrease is determined by:

$$r = k^+ \exp\left(-\frac{E_a}{RT}\right)\prod_i a^{ni}\left[1-\left(\frac{Q}{K}\right)^{\sigma}\right]$$

where r is the dissolution rate, k^+ the forward rate constant, E_a the activation energy, a_i the activity of the i_{th} aqueous species, n_i the corresponding stoichiometric coefficient, Q the ion-activity product of the rate controlling reaction, K the equilibrium constant of the reaction and σ the net reaction order. A simplified version of this expression is:

$$r = r_0\left[1-\left(\frac{Q}{K}\right)^{\sigma}\right]$$

where r_0 is the initial dissolution rate and $1-(Q/K)^{\sigma}$ is an affinity term characterizing the decrease in dissolution rate as the reaction approaches equilibrium. In glass science this simplified expression may be used assuming that the dissolution rate is based on silicon released into solution. A diagram of the corrosion process stages is displayed in Figure 1-2.

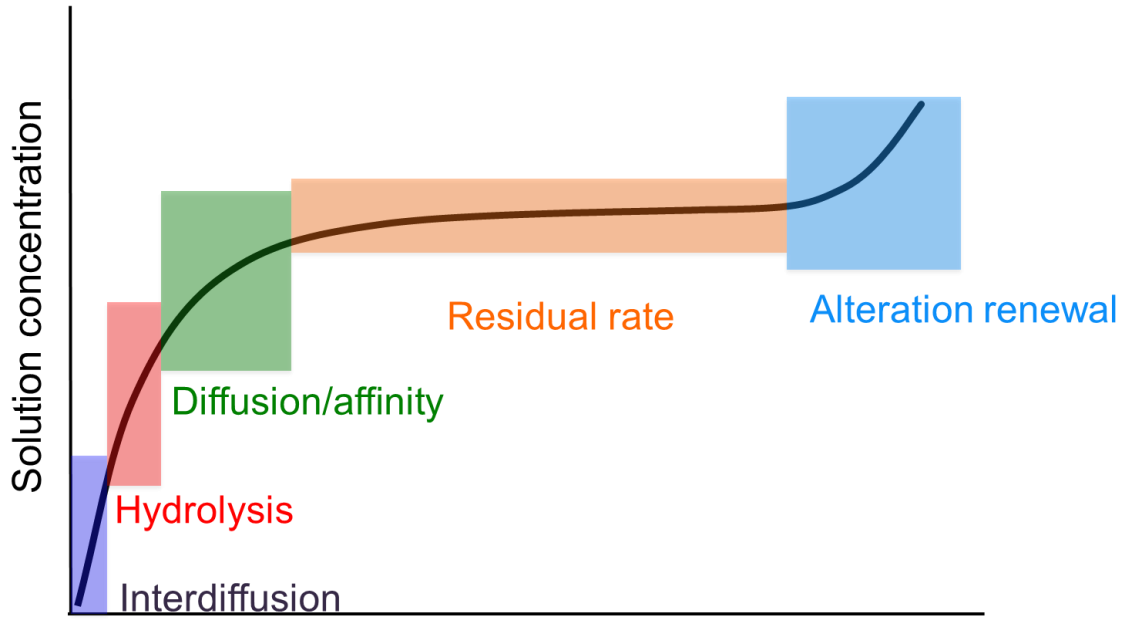

Figure 1-2. Stages of waste glass corrosion process as a function of time.[5]

1.1.4 Formation of Alteration Layer

The second hypothesis used to explain the decrease in corrosion is the formation of a "protective" alteration layer. Extensive studies have shown that in addition to the interdiffusion and hydrolysis reactions occurring at the surface, there are two other interactions: (i) the condensation of sparingly soluble species such as Si, Al, and Ca leading to the formation of a hydrous "gel layer", (ii) precipitation of crystalline phases consisting mostly of clay minerals and rare earth phosphates which occurs at extended periods of time.[6] This macroporous gel layer is thought to act as a diffusion barrier that keeps soluble species such as Si, B, and Na from being further released to solution. However, the precipitation of crystalline phases within the gel or on the gel surface may lead to alteration renewal in which elements continue to be leached from the glass network. The reason for this alteration renewal stage is that when these crystalline phases precipitate on the gel layer, they disturb the thermodynamic equilibrium between elements within the glass network and elements within solution; thus creating a thermodynamic driving force for further dissolution of the glass matrix. An SEM image of this gel alteration layer is displayed in Figure 1-3.

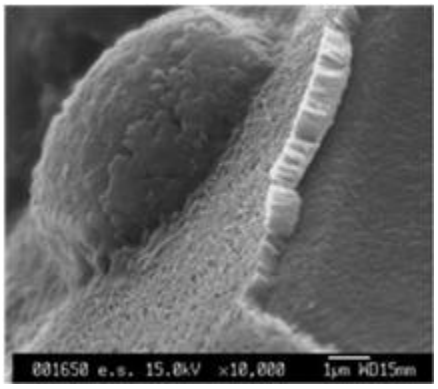

Figure 1-3. SEM image of "gel" alteration layer present on glass surface. This layer is believed to act as a protective diffusion barrier between the glass surface and surrounding environment.[7]

The potential of these layers to be protective is unknown. Previous work by Gin, *et al.* has provided strong support in favor of this alteration layer acting as a protective barrier.[6] Secondary ion mass spectrometry (NanoSIMS) characterization has provided evidence showing that the glass surface can be separated into four distinct layers: pristine glass, hydrated glass layer, gel layer, and crystalline phase layer. This gel layer is characterized by a sharp decrease in the amount of soluble species such as boron and lithium relative to the amount of silicon present as displayed in Figure 1-4. Further evidence of the protective behavior of this alteration layer is displayed from NanoSIMS characterization of a gel cross-section in Figure 1-5. The sharp decrease in the concentration of boron across this tiny cross-section not only shows the complexity of the surface chemistry of glasses, it also describes the precise thickness and location of this boundary at the interface of the glass surface and surrounding environment.

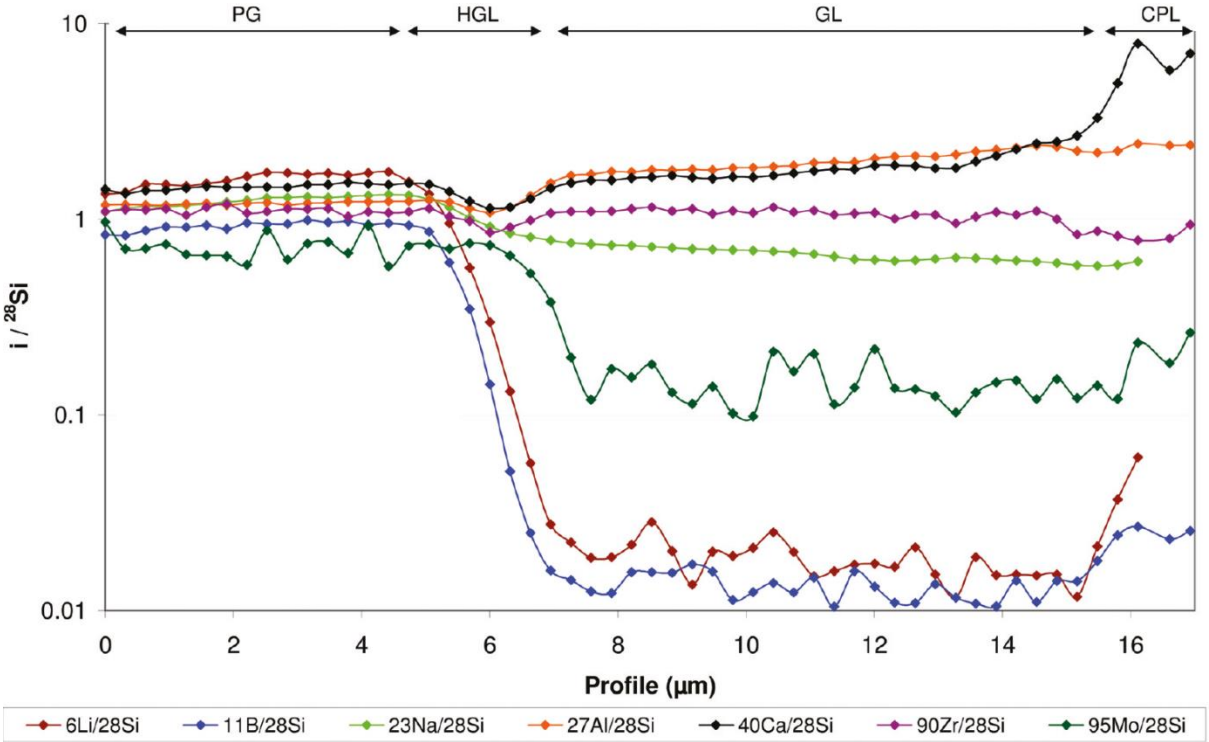

Figure 1-4. NanoSIMS characterization of elements present in waste glass surface layers relative to the amount of silicon present. This profile is taken at varying depths of a cross-section of the glass surface. Labels represent: pristine glass (PG), hydrated glass layer (HGL), gel layer (GL), and crystalline phase layer (CPL).

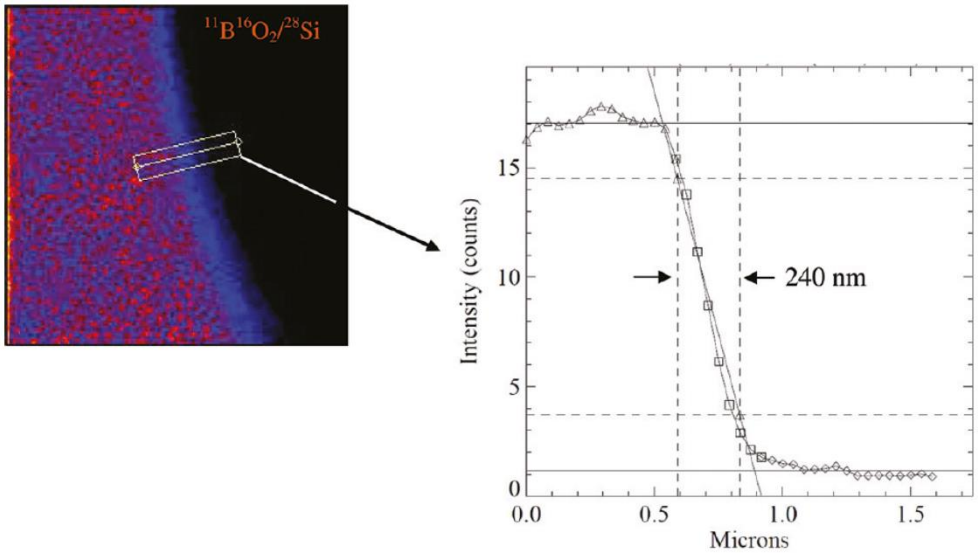

Figure 1-5. NanoSIMS profile of boron gradient present in cross-section of gel layer.

1.1.5 Conclusion

To this point there is still much about the corrosion process that is not understood. Currently scientists are working towards coming to a consensus about the long-term durability of waste glasses. Due to our inability to observe the corrosion behavior of waste glasses over the entire radioactive lifetime of the waste components, scientists instead rely on the use of semi-empirical models to understand the behavior of these borosilicate glasses over long periods of time. If we can successfully characterize the corrosion behavior and long-term durability of nuclear waste glasses over large time scales, nuclear waste vitrification may become the primary method of choice for storing harmful radioactive waste.

Chapter 2

Measuring Variation in Reactive Surface Sites Using Solid-State NMR

2.1 Experiment Theory & Background

2.1.1 Introduction

In order to better describe the behavior of glass during corrosion the relative reactivity should be defined by determining the sites responsible for surface chemistry. The quantification of these sites, therefore, provides a measure of surface reactivity and can be accomplished through attachment of a probe molecule. This study measured the variation in reactive surface sites on nuclear waste glasses under different sets of experimental conditions, which were chosen to promote distinct surface chemistries. The variables selected include pH, corrosion time, and glass composition. ^{19}F solid-state NMR was used as a method for quantifying the reactivity of the probe molecule 3,3,3-(trifluoropropyldimethyl)chlorosilane (TFS) with the surface of different waste glasses in order to measure the reactive surface area of the glass samples.

2.1.2 Reactive Surface Area

One method for quantifying the chemical reactivity of a glass surface is by measuring reactive surface area. There are many different species of silicon present on the glass surface. These different species are given Q^n designations in which Q represents the quaternary silicon atom (tetrahedrally coordinated) and n designates the number of bonds that silicon atom forms with bridging oxygens in the glass network. Previous work by Washton, *et al.* indicates that there

is good agreement between the change in reactive hydroxyls as a function of corrosion rate.[8] A diagram of the different Q^n species present on the glass surface is displayed in Figure 2-1.

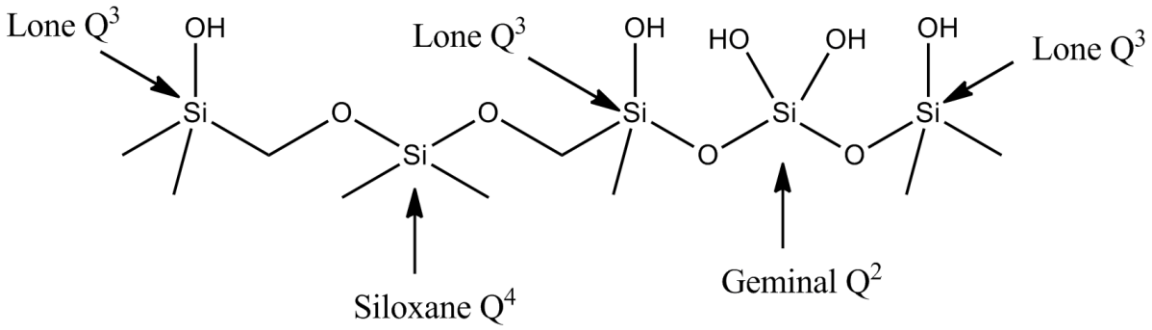

Figure 2-1. Q^n surface sites of waste glasses.

Measuring the reactive surface area of the glass surface is accomplished via attachment of an organic probe molecule to reactive hydroxyls at specific Q^n surface sites. In this study we measure the number of lone Q^3 hydroxyl species in which the silicon is bonded to only one hydroxyl. The reason for interest in this particular species is because previous studies have shown that there is a correlation between the relative number of lone Q^3 reactive sites and the rate-controlling step of dissolution.[8] By determining the relative number of lone Q^3 hydroxyl sites present on the glass surface, we can determine a correlation between the number of lone Q^3 hydroxyl sites and the relative chemical reactivity of the glass surfaces under different corrosion conditions.

2.1.3 TFS Probe Molecule

The selection of an appropriate probe molecule is critical for measuring the reactive surface area of a specific Q^n reactive site. The probe molecule used in this experiment was 3,3,3-(trifluoropropyldimethyl)chlorosilane (TFS) which acts as a mono-functional organosilane. This

probe molecule is mono-functional in that it only has one group that can participate in the condensation reaction. TFS will react primarily with lone Q^3 hydroxyl sites as opposed to other Q^n sites because the hydrogen bonding of Q^2 and Q^3 species is too strong to be overcome during the condensation reaction. Attachment of TFS to lone Q^3 hydroxyls occurs via a two-step mechanism. The first step is a hydrolysis reaction in which the chlorine atom is removed from the TFS molecule and replaced with a hydroxyl. The second step in the mechanism is a condensation reaction occurring between the hydroxyl groups present on the TFS molecule as well as the lone Q^3 reactive site. The TFS molecule as well as the mechanism of attachment is displayed in Figure 2-2.[8]

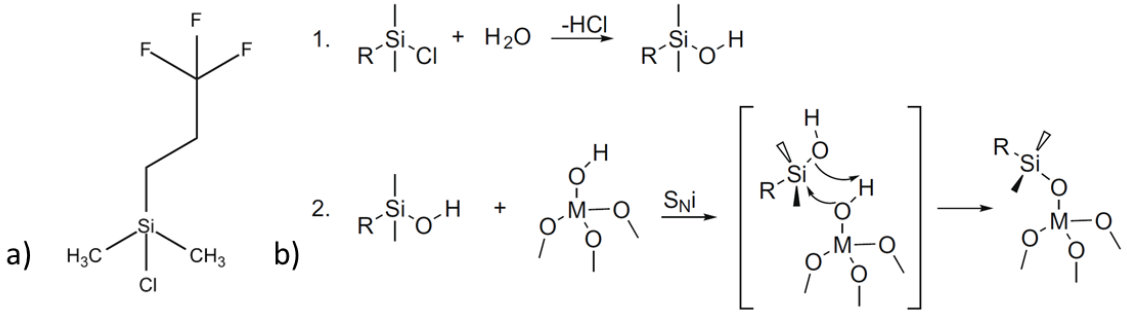

Figure 2-2. a) TFS molecule b) Mechanism of TFS attachment to lone Q^3 hydroxyl.

The ability to quantify the relative proportion of TFS molecules that have attached to the glass surface enables the number of lone Q^3 silicon hydroxyl sites to also be determined. Each molecule of TFS contains three fluorine atoms which can be detected by magic angle spinning nuclear magnetic resonance (MAS NMR). ^{19}F MAS NMR is easily accomplished due to the large gyromagnetic ratio (40.053 MHz T^{-1}) of ^{19}F and its high natural abundance.

2.1.3 Simulated Waste Glass Samples

The glasses of interest in this study were two simulated nuclear waste glasses called SA1R and SS2R. These glasses are models for the American AFCI and French SON68 respectively, and differed in their composition. One of the focuses of this study was to compare the variation in reactive sites as a function of surface area, which was controlled by utilizing different particle sizes. Powder samples of particle sizes 20-32 μm and 75-125 μm were observed under the same leaching conditions in order to measure the variation in reactive surface sites as a function of the total surface area of the glass. Powder particles often contain surface defects as a result of the mechanical stress placed on them during the grinding process as displayed in Figure 2-3. As a result, comparisons of glass powder and fiber were made for the SS2R composition. Glass fibers are known to produce thick surface layers, which should result in a significant proportion of reactive surface sites. Moreover, glass fibers are not subject to the same mechanical stress during production and thus have a more pristine surface than their glass powder counterparts.

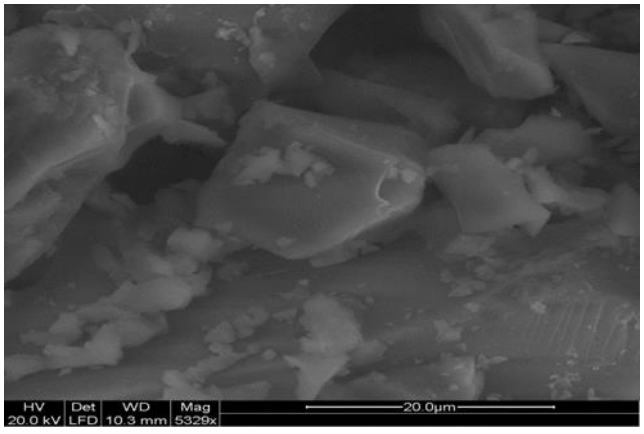

Figure 2-3. SEM image of 20 μm glass powder particles.[9]

2.1.4 Buffer Systems

Three buffer solutions (pH 4, 7 and 11) were produced in order to study the nature of the gel layers (i.e. thickness, composition) under different corrosion regimes. The components of these buffers were chosen in order to generate difference surface chemistries which should resonate as deviations in the number of reactive surface sites. We are also trying to determine the number of reactive surface sites for different pH values that have been used in previous corrosion studies. The selection of pH values in these previous experiments is to determine the difference in corrosion behavior as a function of pH. The composition of these buffer systems is found in Table 2-1. The pH values were chosen based off of common pH values used in previous corrosion studies. The TRIS buffer in particular is a commonly used buffer in corrosion studies due to its stability over long periods of time and inertness with respect to other constituents in solution.[10]

Table 2-1. Chemical Components of Buffer Systems

Solution pH	Buffer Components
4	sodium acetate (CH_3COONa) and acetic acid (CH_3COOH)
7	tris(hydroxymethyl)aminomethane (TRIS) and hydrochloric acid (HCl)
11	potassium bicarbonate ($KHCO_3$) and potassium hydroxide(KOH)

2.1.6 Nuclear Magnetic Resonance

Some nuclei possess both spin and charge and thus also have a magnetic dipole moment associated with them, however, not all nuclei are NMR active. Only nuclei with a non-zero spin can be detected through NMR. In the absence of a magnetic field the nuclear energy levels of these nuclei are degenerate. When a magnetic field is applied degeneracy is broken and the nuclei

can occupy one of 2I+1 spin states in which I represents the spin quantum number of the given nuclei. The value of these energy levels is given by:

$$E_m = -m\hbar\gamma B_0$$

where m is the substate, $\hbar$ is planck's constant, B_0 is the strength of the magnetic field, and γ is the gyromagnetic ratio of the nuclide.[11]

When placed in a magnetic field at room temperature there is a slight abundance of nuclei in the lower energy state compared to the higher energy state as seen in Figure 2-4. This abundance equates to approximately a few spins per 1000 nuclei at room temperature. The population between any two energy levels is given by a Boltzmann distribution:

$$\frac{N_m}{N} = \frac{\exp\left(-E_m / kT\right)}{\sum_n \exp\left(-E_n / kT\right)}$$

The strength of the signal observed through NMR is proportional to the relative abundance and gyromagnetic ratio of the nuclide of interest. These factors make NMR a low-sensitive technique compared to other spectroscopic methods which detect greater differences in energy.

Each individual nuclide precesses about the magnetic field at a specific resonance frequency known as its Larmor frequency. When an RF pulse at the Larmor frequency is applied along a direction perpendicular to the magnetic field the nuclei will undergo transitions between substates. The RF pulse also promotes coherent motion of the nuclear spins, causing them to align. When this RF pulse is applied the net magnetization vector of the nuclei will tip at an angle (in radians) proportional to the strength and duration of the applied pulse:

$$\theta = \gamma B_1 \tau_p$$

A typical one-pulse NMR experiment will consist of applying a 90° pulse such that the net magnetization is rotated into the xy-plane. A typical NMR spectrometer will measure the decay

of transverse magnetization; therefore the signal observed during an NMR experiment is maximized when the net transverse magnetization is greatest in the xy-plane. The decay of this transverse magnetization within the xy-plane is measured by an RF coil and is the signal observed in a nuclear magnetic resonance experiment. The number of a given spin present in a sample can be determined by comparing the intensity of the NMR signal for the sample to that of a standard with a known number of those nuclides. For the purposes of our study we are interested in measuring the number of ^{19}F atoms present in our sample, relative to a standard of sodium trifluoroacetate (NaTFA) diluted in silica gel, in order to determine the relative number of lone Q^3 hydroxyl sites that are present on the glass surface.

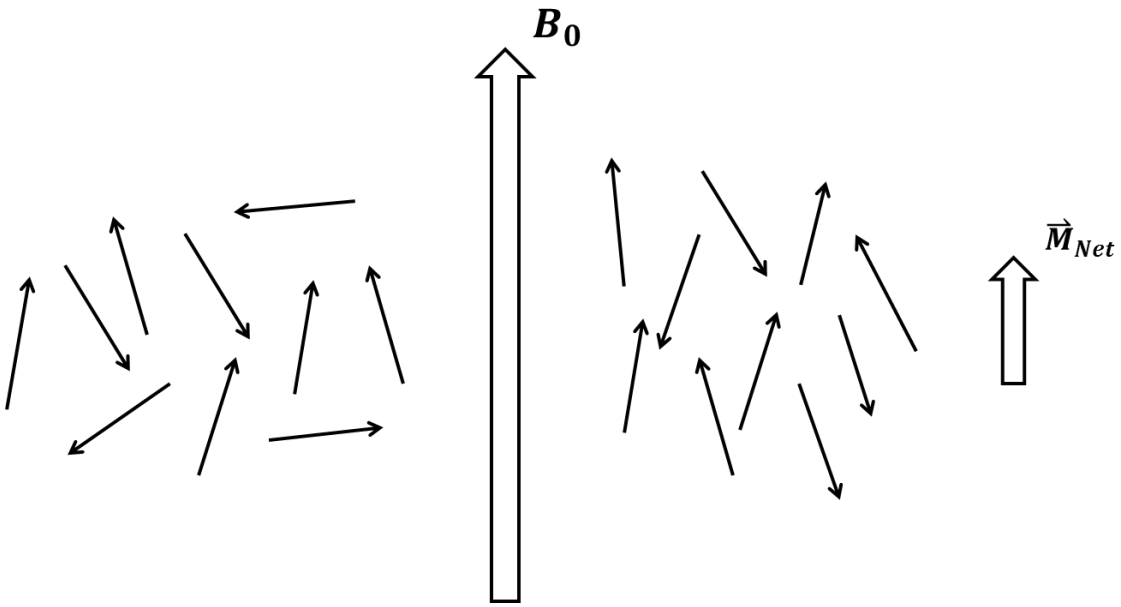

Figure 2-4. Diagram representing the degeneracy of the nuclei breaking once a magnetic field is applied. At room temperature there is a slight abundance of nuclei in the lower energy state (parallel to direction of magnetic field) than the higher energy state (antiparallel to direction of magnetic field) which produces a net magnetization vector.

2.2 Experimental Procedure

2.2.1 Overview

The experimental parameters that were varied during the studies presented here include solution composition, particle size, and total corrosion time. For each glass species a summary of the experimental variables is found in Figure 2-5. The purpose of these combinations was to modify each of the corrosion variables, while holding the others constant, in order to observe the changes they caused in the reactivity of the glass with respect to its surrounding environment. By modifying the corrosion variables we expect to observe changes in the surface chemistry of the glass including corrosion behavior and thickness of the formed alteration layer.

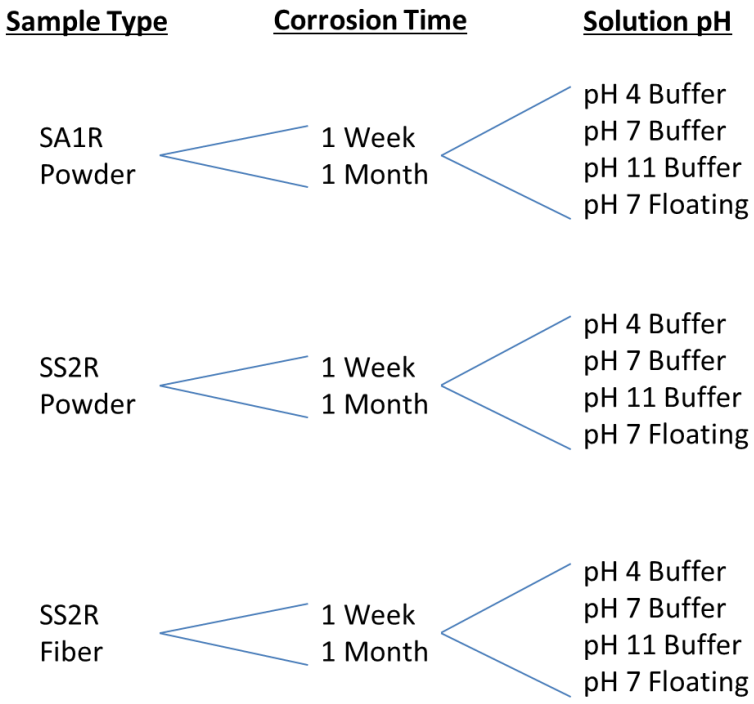

Figure 2-5. Diagram of different combinations of corrosion parameters

2.2.2 Preparation of Glass Samples

Glasses were made in 200 g batches. The melting conditions included a temperature of 1275°C and one hour duration. The resulting molten mixture was supercooled by quench pouring, crushed and remelted at 1275°C for better sample homogeneity. The glass powder was crushed to particle sizes between 75-125 μm and 20-32 μm. The glass powder then underwent a rinsing procedure to remove any fine particles still present on the powder. The rinsing procedure consisted of suspending the crushed powder in ASTM Type I water and sonicating it for a period of two minutes in order to break up any remaining fine particles. After the two minutes had passed the powder was left undisturbed for a period of one minute in order to allow the larger particles to settle to the bottom of the vial. Once that time had passed the liquid containing the fine particles was decanted and the procedure was repeated for a total three rinses with ASTM Type I water and two rinses with ethanol.[12] After the procedure was complete the rinsed powder was placed into an oven at 90°C overnight for drying.

2.2.3 Corrosion Conditions

The leaching solutions for this study consisted of three buffer systems as well as a non-buffered, floating solution. The components of the buffer solutions are seen in Table 2-2. The non-buffered solution had a natural pH of 7 and consisted of ASTM Type I water which has very low concentrations of silicon. This ensures that our leaching solution is relatively free of silicon species that could participate in recondensation reactions that interfere with the results of this study. For the powder samples the BET surface area-to-solution volume ratio was 100,000 m^{-1} and for the fiber samples the ratio was 10,000 m^{-1}. These ratios were chosen in order to ensure

that a sufficient amount of alteration occurred to the glass surface during the given time periods of the experiment. The BET surface areas for each glass are found in Table 2-2.

Table 2-2. BET Surface Areas of Waste Glasses (N_2 adsorption gas)

Glass & Particle Size	BET Surface Area (m^2/g)
SA1R 20-32 µm	0.33
SA1R 75-125 µm	1.60
SS2R 20-32 µm	0.58
SS2R 75-125 µm	0.47

Two grams of the glass powders, or one gram of the glass fiber, and the appropriate volume of corrosion solution were placed into perfluoroalkoxy (PFA) bottles before then being placed in an oven at 90°C. The purpose of these high temperatures was to increase the corrosion rate so that an appreciable amount of corrosion can be observed during the desired corrosion time. Once the samples were removed from the oven they were weighed to account for potential solution loss, or glass powder dissolution. The powder samples were then filtered via vacuum filtration, rinsed with water to remove any residual buffer, and left in the hood overnight to allow the samples to equilibrate with the air. The dry leached samples were weighed out into triplicates (0.5 grams for powder samples, 0.25 grams for fiber samples) in preparation for TFS treatment.

2.2.4 TFS Treatment

Prior to TFS treatment the samples were placed in a vacuum oven for a period of 12 hours at 160°C. This was to ensure that any water molecules that could possibly interfere with TFS attachment were removed from the surface. The samples were then removed from the oven and placed into Schlenk flasks along with 25 mL of anhydrous toluene to act as a solvent. 1 mL

of TFS was added in excess to ensure that all lone Q^3 Si hydroxyls on the glass surface were able to react with the probe molecule. These flasks were then sealed, pulled under vacuum and back-filled with argon gas before being placed into a shaker bath for a period of 72 hours. Once the 72 hours had passed the samples were filtered via vacuum filtration and placed in a vacuum oven for a period of one hour at 120°C. The boiling point of TFS is 118°C; therefore that oven temperature will ensure that any excess liquid TFS remaining on the glass surface will be boiled off. Once the samples were removed from the vacuum oven they were ready to undergo NMR analysis.

2.2.5 ^{19}F MAS SSNMR Analysis

All NMR experiments in this study were performed on a 400 MHz NMR spectrometer utilizing an Oxford 9.4 T magnet and Tecmag data acquisition system. Radiofrequency $\pi/2$ pulses of 9.5 μs were used with a pre-pulse delay of 5 s. MAS spinning frequencies of 10 kHz were used with a 4mm Chemagnetics double resonance probe tuned to the ^{19}F resonance frequency of 376.346 MHz in order to acquire direct polarization data from between 4,000 and 20,000 transients. $CFCl_3$ was used as a reference in determining the chemical shift of TFS. NMR data were processed using NUTS NMR data processing software from Acorn NMR.

Chapter 3

Results & Discussion

3.1 Results

The overall objective of this study was to observe variations in the number of reactive surface sites (defined here as the number of lone Q^3 silicion hydroxyl sites) as a function of particle size, solution pH, corrosion time, and glass composition. All values are listed on a per gram of glass material basis. A summary of the experimental results is displayed in Table 3-1.

Table 3-1. Experimental results reported as number of lone Q^3 hydroxyls per gram of glass material.

SA1R Glass

SA1R 20-32µm 1 Week

Solution	Average OH/g
pH 4 Buffered	$4x10^{17} \pm 2x10^{17}$
pH 7 Buffered	$1.1x10^{17} \pm 0.3x10^{17}$
pH 11 Buffered	$2.3x10^{17} \pm 0.6x10^{17}$
pH 7 Floating	$5.2x10^{17} \pm 0.1x10^{17}$

SA1R 20-32µm 1 Month

Solution	Average OH/g
pH 4 Buffered	$2.3x10^{17} \pm 0.8x10^{17}$
pH 7 Buffered	$2.6x10^{17} \pm 0.5x10^{17}$
pH 11 Buffered	$3.3x10^{17} \pm 0.5x10^{17}$
pH 7 Floating	$3.4x10^{17} \pm 0.8x10^{17}$

SA1R 75-125µm 1 Week

Solution	Average OH/g
pH 4 Buffered	$7x10^{16} \pm 1x10^{16}$
pH 7 Buffered	$7x10^{16} \pm 2x10^{16}$
pH 11 Buffered	$3x10^{17} \pm 2x10^{17}$
pH 7 Floating	$1.7x10^{17} \pm 0.7x10^{17}$

SA1R 75-125µm 1 Month

Solution	Average OH/g
pH 4 Buffered	$1.6x10^{17} \pm 0.2x10^{17}$
pH 7 Buffered	$1.0x10^{17} \pm 0.1x10^{17}$
pH 11 Buffered	$1.32x10^{17} \pm 0.08x10^{17}$
pH 7 Floating	$3.1x10^{17} \pm 0.2x10^{17}$

SS2R Glass

SS2R 20-32µm 1 Week

Solution	Average OH/g
pH 4 Buffered	$2.1x10^{17} \pm 0.9x10^{17}$
pH 7 Buffered	$2x10^{17} \pm 1x10^{17}$
pH 11 Buffered	$6x10^{17} \pm 1x10^{17}$
pH 7 Floating	$4.72x10^{17} \pm 0.08x10^{17}$

SS2R 20-32µm 1 Month

Solution	Average OH/g
pH 4 Buffered	$7.5x10^{17} \pm 0.6x10^{17}$
pH 7 Buffered	$8x10^{17} \pm 6x10^{17}$
pH 11 Buffered	$7x10^{17} \pm 7x10^{17}$
pH 7 Floating	$4.0x10^{17} \pm 0.8x10^{17}$

SS2R 75-125µm 1 Week

Solution	Average OH/g
pH 4 Buffered	$1.3x10^{17} \pm 0.4x10^{17}$
pH 7 Buffered	$8x10^{16} \pm 2x10^{16}$
pH 11 Buffered	$1.9x10^{17} \pm 0.7x10^{17}$
pH 7 Floating	$2.8x10^{17} \pm 0.2x10^{17}$

SS2R 75-125µm 1 Month

Solution	Average OH/g
pH 4 Buffered	$1.4x10^{18} \pm 0.4x10^{18}$
pH 7 Buffered	$1.9x10^{17} \pm 0.3x10^{17}$
pH 11 Buffered	$2.2x10^{17} \pm 0.8x10^{17}$
pH 7 Floating	$1.8x10^{17} \pm 0.3x10^{17}$

SS2R Fiber 1 Week

Solution	Average OH/g
pH 4 Buffered	$7x10^{17} \pm 2x10^{17}$
pH 7 Buffered	$3.8x10^{17} \pm 0.8x10^{17}$
pH 11 Buffered	$4.9x10^{17} \pm 0.4x10^{17}$
pH 7 Floating	$9x10^{17} \pm 2x10^{17}$
Nonleached	$5.3x10^{17} \pm 0.7x10^{17}$

SS2R Fiber 1 Month

Solution	Average OH/g
pH 4 Buffered	$5.4x10^{17} \pm 0.9x10^{17}$
pH 7 Buffered	$1.9x10^{17} \pm 0.3x10^{17}$
pH 11 Buffered	$1.0x10^{18} \pm 0.6x10^{18}$
pH 7 Floating	$1.1x10^{18} \pm 0.2x10^{18}$
Nonleached	$5.3x10^{17} \pm 0.7x10^{17}$

3.2 Discussion

Based on the results of the study, we can make certain hypotheses regarding the surface chemistry of simulated waste glasses. Several trends can be ascertained from these data that provide enlightenment about glass corrosion. In general, the pH 7 floating solution produced higher OH/g values than the buffered solutions. Previous studies have shown that the dissolution rate of waste glasses increases with increasing pH at constant temperatures.[13] Washton, *et al.*

demonstrated that there is a direct correlation between the dissolution rate of glasses and the number of reactive lone Q^3 surface hydroxyls.[8] Therefore, we would expect to observe an increase in the number of lone Q^3 hydroxyls as a function of increasing pH of the corrosion solution. In many of our pH 7 buffered sample sets we observe a lower than expected increase in OH/g relative to the observed number of OH/g in our pH 4 buffered samples. Due to a lack of consistency between results and expected trends, we hypothesize that another factor must be affecting corrosion. For example, it is possible that interactions are occurring between the buffer systems and glass surface which would block corrosion sites.

The buffer components chosen in this study simulate a variety of corrosion conditions which are observed in various pH ranges. The TRIS/HCl buffer in particular is one of the most commonly used corrosion buffers in glass science.[10] Previous work has shown that it is possible for certain organic molecules, such as acetic acid (the chemical utilized in the pH 4 system), to adsorb to the surface of aluminoborosilicate glasses as displayed in Figure 3-1.[14]

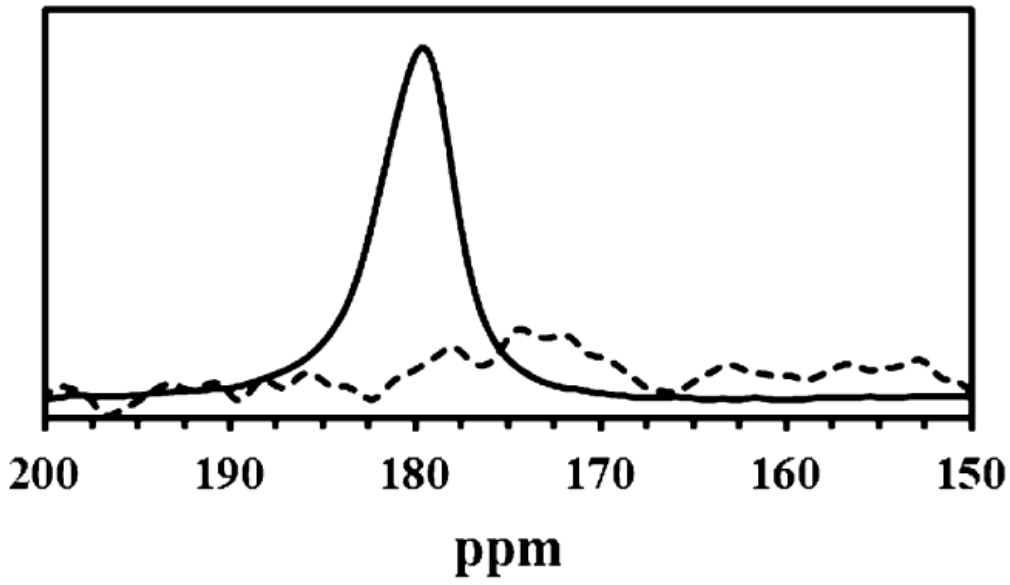

Figure 3-1. ^{13}C NMR spectra of aluminoborosilicate fiber indicating attachment of acetic acid to the glass surface (180 ppm peak, solid line)[14]

If this is the case with the components of our buffer solutions, we may observe a difference in the measured number of OH/g compared to the true value. It is possible that these buffer solutions, particularly the TRIS buffer, may be forming hydrogen bonds with the glass surface that could block glass corrosion sites. In many sample sets the TRIS buffer produced lower than expected OH/g values compared to what we would expect based on the OH/g values for the pH 4 buffer sets. This may be attributed to the bulkiness of the molecule as well as its ability to form multiple hydrogen bonds with the glass surface. A diagram of the chemical structure of TRIS is displayed in Figure 3-2.

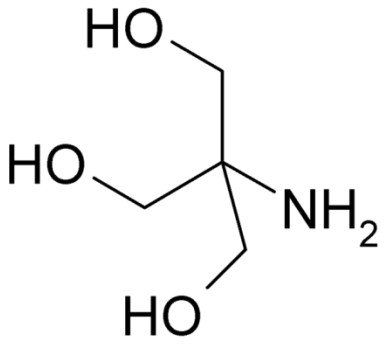

Figure 3-2. Chemical structure of tris(hydroxymethyl)aminomethane (TRIS). The hydroxyl group and amine sites have the potential to form hydrogen bonds with hydroxyls present on the glass surface.

Furthermore, we found that in nearly every sample set the pH 7 floating samples produced higher OH/g values than both the pH 7 buffered samples and pH 11 buffered samples. This observation provides more evidence that buffer components may be blocking corrosion sites. Further support for the blocking of Q^3 silicon hydroxyl sites can be observed in the SS2R fiber samples. The nonleached fibers have not been exposed to any solution and therefore are expected to produce lower OH/g values than the corroded fibers since corrosion generates surface hydroxyl groups. We found that our nonleached fiber samples yielded higher OH/g values than the TRIS buffer samples. This result suggests that there may be some interaction occurring between the

buffer components of the corrosion solutions and the glass surface which may be blocking glass corrosion sites.

In general, the pH 11 buffer tended to produce higher OH/g values than the pH 4 and pH 7 buffer solutions. This result is expected based off our predictions; however, it is expected that the surface layers formed at various pH values differ. The pH value of 11 was chosen due to the similarities in equilibrium pH for the glasses utilized in this study. In glass corrosion the equilibrium pH represents the constant pH value reached as a glass undergoes dissolution and is dependent upon the composition of the glass. Under more basic conditions we would also expect the gel layer to contain more components from the bulk glass material as opposed to acidic conditions in which the gel layer consists primarily of silica gel.

One would expect longer corrosion times to produce higher OH/g values than shorter corrosion times due to increased exposure of the glass surface to solution, resulting in enhanced corrosion. We find for the SS2R powder samples this hypothesis holds true. However, for the SS2R fiber and SA1R powder samples we find that in certain sample sets the one week samples produced higher OH/g values than the one month samples. The decrease in lone Q^3 hydroxyls as a function of corrosion time may be due in part to reformation of bridging oxygen bonds with the bulk glass through recondensation, which is believed to be one mechanism responsible for the formation of alteration layers. Recondensation results from silicic acid in solution reforming bridging oxygen bonds with the bulk glass surface as the acid becomes saturated in solution.[15] Although we expect that that the glass is still corroding under longer corrosion times, the decrease in the observed number of OH/g in these samples may be attributed to the transformation of Q^3 sites to Q^4 sites as these Q^3 species undergo recondensation to form siloxane groups. This process by which lone Q^3 silicon species undergo a transformation to Q^4 species is displayed in Figure 3-3.

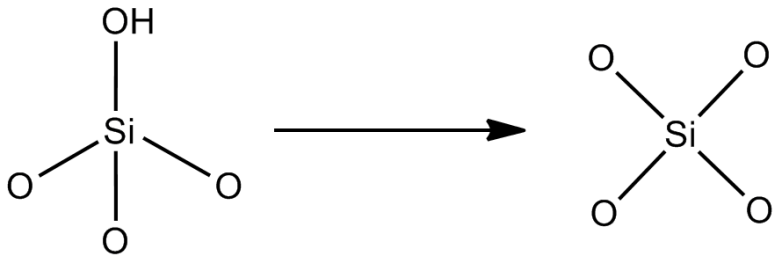

Figure 3-3. Transformation of Q^3 silicon species to Q^4 as the silicon reforms bridging oxygen bonds with the bulk glass.

From our results we can also hypothesize that this process occurs faster with the SA1R glass powders than the SS2R glass powders. However, other factors may also be responsible.

On a per gram basis we would expect to observe higher OH/g values for the 20-32 µm powder particles than the 75-125 µm powder particles due to the higher surface area as displayed in Table 2-2. In the vast majority of our samples we found that this expectation holds true. We also note that in the majority of our samples the SS2R glass powder produced higher OH/g values than the SA1R powder samples. These data indicate that the nature of the alteration layers in these samples differs. If the differences in these alteration layers affects the corrosion rate of these samples, this could have important implications regarding the durability of these compositions.

Due to the large standard deviations in OH/g within sample sets, particularly the SS2R 20-32 µm 1 month pH 7B and pH 11B sample sets, it is necessary that we address possible reasons for this variation. Q-tests are one method for removing outliers from a data set by obtaining a ratio of the difference in value between a suspected outlier and the next nearest value in the sample set over the total range of the entire sample set. Using a 95% confidence limit we determined no outliers were present in any of our sample sets via a Q-test. We observe that in general the SS2R fiber samples yielded lower standard deviation values than the SS2R powder samples. This can most likely be attributed to the presence of surface defects in the SS2R

powders resulting from the grinding process. Determining the source for the large standard deviations between the different powder samples will be investigated in future studies.

One potential source for the large standard deviations observed in the powder samples may be attributed to the appearance of a second peak in our ^{19}F NMR spectra. The typical chemical shift for chemisorbed (chemically bonded) TFS appears at -68 ppm. In many of our samples, we also see the appearance of a second peak at -62 ppm. This represents the chemical shift of pure liquid TFS. There are two potential explanations for the observation of the second peak. Liquid TFS may become trapped in the pores of the gel layer, preventing it from being evaporated during heating. The gel layer itself is macroporous with pore sizes large enough for TFS to become trapped within them.[16] The second possibility is that TFS is physisorbed to the glass surface, likely through hydrogen bonding of the hydroxyl surface sites and the –OH on the hydrolyzed TFS molecule.[17] The strength of this interaction would be too great to be overcome by the currently utilized heating regime.

In both scenarios the TFS molecule would show up at the same chemical shift as pure liquid TFS as charge density would not be affected. Due to the overlap between the two resonances, separation by deconvolution was difficult and prevented the removal of the higher frequency resonance from OH/g determinations. The intensity of the higher frequency resonance varied greatly between sample sets and even within TFS triplicates, which likely accounts for some of the large standard deviations observed in our samples. Future work will be required to determine the source of variation in physisorbed TFS between samples. A sample ^{19}F NMR spectrum showing both peaks is displayed in Figure 3-4.

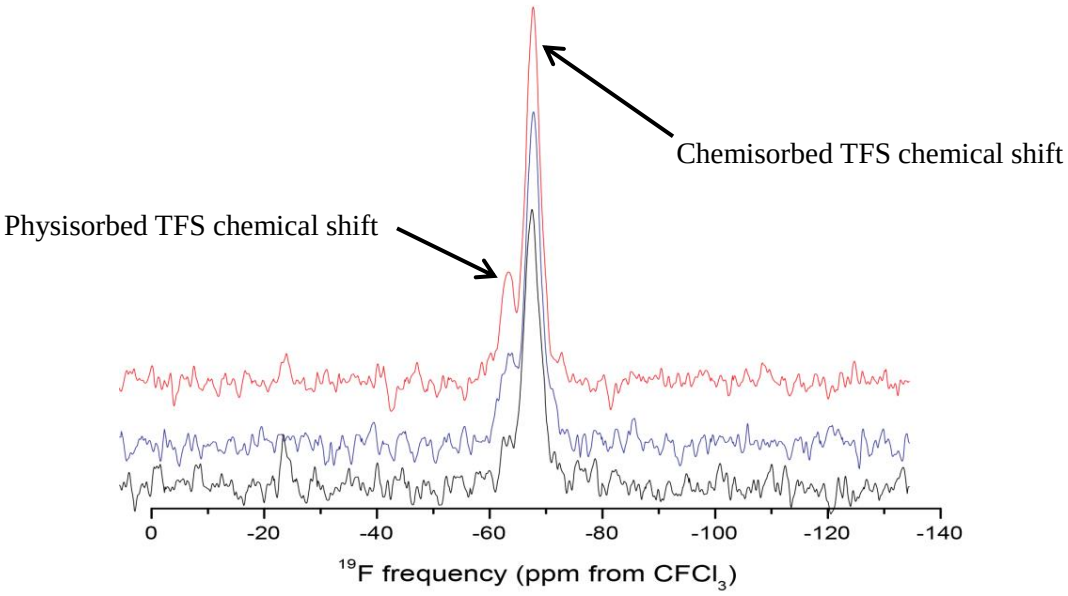

Figure 3-4. Sample ^{19}F NMR spectra of SA1R 20-32 μm 1 month pH 7 floating sample. The peak at -68 ppm represents TFS attachement while the peak at -62 ppm represents physisorbed TFS.

3.3 Conclusion

From the results of our study we can establish several trends regarding the corrosion of waste glasses. In general, we find that the observed number of OH/g increases with decreasing particle size as would be expected due to the increase in total surface area of the glass. We also found that in general the number of OH/g increases with respect to increasing pH of the corrosion solution. This result implies that the nature of the alteration layers differs as a function of the pH value of the corrosion solution.

Characterizing the change in surface sites with respect to longer exposure times is more difficult. We find that for the SS2R powder samples the one month samples all produced higher OH/g values than the one week samples, however, for the SS2R fiber and SA1R powder we found more variation in the OH/g values as a function of corrosion time. The lack of increase in

OH/g for SA1R and SS2R powders suggest that the surface chemistry of these glasses is complex and does not follow a trend that Q^3 sites will increase with exposure time. This indicates that a combination of reactions is responsible for the formation and maturation of the gel layer. Perhaps the most interesting observation in this study is the potential interaction of the buffer systems with the waste glass surfaces indicated by our measured OH/g values for each pH solution. Additional experiments are required to confirm this hypothesis and determine the extent of interaction.

REFERENCES

1. Ojovan, M. I.; Lee, W. E., Glassy Wasteforms for Nuclear Waste Immobilization. *Metallurgical and Materials Transactions a-Physical Metallurgy and Materials Science* **2011,** *42A* (4), 837-851.

2. Grambow, B., Nuclear waste glasses - How durable? *Elements* **2006,** *2* (6), 357-364.

3. Overview of Waste Glass Formation. In *Washington State Department of Ecology*.

4. Van Iseghem, P.; Aertsens, M.; Gin, S.; Deneele, D.; Grambow, B.; McGrail, P.; Strachan, D.; Wicks, G. *Glamor: A Critical Evaluation of the Dissolution Mechanisms of High Level Waste Glasses in Conditions of Relevance for Geologic Disposal*; European Comission: 2007.

5. Murphy, K., Waste Glass Corrosion Process.

6. Gin, S.; Guittonneau, C.; Godon, N.; Neff, D.; Rebiscoul, D.; Cabie, M.; Mostefaoui, S., Nuclear Glass Durability: New Insight into Alteration Layer Properties. *Journal of Physical Chemistry C* **2011,** *115* (38), 18696-18706.

7. Ribet, S.; Gin, S., Role of neoformed phases on the mechanisms controlling the resumption of SON68 glass alteration in alkaline media. *Journal of Nuclear Materials* **2004,** *324* (2-3), 152-164.

8. Washton, N. M.; Brantley, S. L.; Mueller, K. T., Probing the molecular-level control of aluminosilicate dissolution: A sensitive solid-state NMR proxy for reactive surface area. *Geochimica Et Cosmochimica Acta* **2008,** *72* (24), 5949-5961.

9. Murphy, K., SEM image of 20 micron glass particle.

10. Tournie, A.; Majerus, O.; Lefevre, G.; Rager, M. N.; Walme, S.; Caurant, D.; Barboux, P., Impact of boron complexation by Tris buffer on the initial dissolution rate of borosilicate glasses. *Journal of Colloid and Interface Science* **2013,** *400*, 161-167.

11. Jarvie, T. P.; Mueller, K. T., Advances in Analytical Geochemistry. In *Advances in Analytical Geochemistry*, JAI Press Inc.: 1995; pp 141-240.

12. Standard Test Methods for Determining Chemical Durability of Nuclear, Hazardous, and Mixed Waste Glasses and Multiphase Glass Ceramics: The Product Consistency Test (PCT). ASTM International.

13. Mazer, J. J.; Walther, J. V., DISSOLUTION KINETICS OF SILICA GLASS AS A FUNCTION OF PH BETWEEN 40 AND 85-DEGREES-C. *Journal of Non-Crystalline Solids* **1994,** *170* (1), 32-45.

14. Stapleton, J. J.; Suchy, D. L.; Banerjee, J.; Mueller, K. T.; Pantano, C. G., Adsorption Reactions of Carboxylic Acid Functional Groups on Sodium Aluminoborosilicate Glass Fiber Surfaces. *Acs Applied Materials & Interfaces* **2010,** *2* (11), 3303-3309.

15. Valle, N.; Verney-Carron, A.; Sterpenich, J.; Libourel, G.; Deloule, E.; Jollivet, P., Elemental and isotopic (Si-29 and O-18) tracing of glass alteration mechanisms. *Geochimica Et Cosmochimica Acta* **2010,** *74* (12), 3412-3431.

16. Cailleteau, C.; Angeli, F.; Devreux, F.; Gin, S.; Jestin, J.; Jollivet, P.; Spalla, O., Insight into silicate-glass corrosion mechanisms. *Nature Materials* **2008,** *7* (12), 978-983.

17. Fry, R. A.; Mueller, K. T.; Pantano, C. G., Effect of boron oxide on surface hydroxyl coverage of aluminoborosilicate glass fibres: a F-19 solid state NMR study (vol 44, pg 64, 2003). *Physics and Chemistry of Glasses* **2004,** *45* (3), 222-222.

ACADEMIC VITA

DANIEL P. BANKS

601 Vairo Boulevard Apt. 233, State College, PA 16803 | 610-621-6010 | dpb5125@psu.edu

EDUCATION

Penn State University (Schreyer Honors College), University Park, PA

B.S. Honors in Chemistry **Spring 2014**

Honors in Physics

SCHOLARSHIPS AND AWARDS

Elizabeth and J. Paul Smith Scholarship	2013
George G. Pond Memorial Scholarship	2012
Faculty Fund Research Grant Recipient	2012, 2013
Penn State Berks Outstanding Achievement Award – Organic Chemistry	2012
Penn State Berks Outstanding Achievement Award – Physics	2012

RESEARCH EXPERIENCE

Penn State University

Undergraduate Research Assistant in Chemistry, Mueller Research Group **2012 –2014**

Applied ^{19}F solid-state magic angle spinning NMR to leached simulated nuclear waste glasses as a method for quantifying the surface reactivity of these glasses. Responsible for producing glass samples, carrying out leaching experiments under different sets of simulated environmental conditions, and applying ^{19}F SSNMR to measure the relative number of lone Q^3 hydroxyls per gram via attachment of a fluorine-containing probe molecule. Worked under the direction of Dr. Karl T. Mueller.

Penn State University

Undergraduate Research Assistant in Physics **2011 – 2014**

Responsible for calculating the probability distribution of quarks in nucleons as a function of their transverse momentum. Used Mathematica to simplify transverse momentum functions to their most basic form before using an integration routine in Fortran to compute the probability distribution values of transverse momentum integrals. Worked under direction of Dr. Leonard P. Gamberg.

Thomas Jefferson National Accelerator Facility, Newport News, VA

Summer Undergraduate Laboratory Intern (SULI) with U.S. Department of Energy **2012**

Optimized the power output and optics of industrial diode lasers in order to maximize the transfer of atomic spin polarization from rubidium and potassium atoms to the nuclear spin of He-3 atoms in spin-exchange optical pumping process. Measured the magnitude of this polarization using a rudimentary nuclear magnetic resonance (NMR) and electron paramagnetic resonance (EPR) system built at Jefferson Lab. Worked under supervision of Dr. Jian-Ping Chen.

TEACHING EXPERIENCE

Penn State University

Chemistry Tutor **Fall 2012**

One semester of experience as a chemistry tutor for general chemistry and organic chemistry.

Teaching Assistant – Chem 112: Chemical Principles II **2011 – 2012**

Three semesters of experience as a teaching assistant for second semester course in general chemistry. Assisted instructor in facilitating students' comprehension of course material. Held review sessions and graded exams.

Teaching Assistant – Chem 110: Chemical Principles I **2011-2012**

Two semesters of experience as a teaching assistant for first semester course in general chemistry. Assisted instructor in facilitating students' comprehension of course material. Held review sessions and graded exams.

Teaching Assistant- Chem 101: Introductory Chemistry **Spring 2012**

One semester of experience as a teaching assistant for an introductory chemistry course for non-science majors. Assisted instructor in facilitating students' comprehension of course material. Held review sessions and graded exams.

CONFERENCES AND PRESENTATIONS

"The Beam-Spin Asymmetry and T-Odd Effects"
Poster presented at annual American Physical Society Division of Nuclear Physics conference, Newport News, VA 2013

"Probing the Reactive Surface of Nuclear Waste Glass Using Solid-State NMR"
Poster presented at American Chemical Society local chapter undergraduate research symposium, University Park, PA 2013

"Modeling Internal Structure of Nucleon"
Poster presented at annual American Physical Society Department of Nuclear Physics conference, Newport Beach, CA 2012

MEMBERSHIPS

American Chemical Society